Study on Ultra-Structural Effects Caused by Onion yellow dwarf virus Infection in 'Rossa di Tropea' Onion Bulb by Means of Magnetic Resonance Imaging.

Anna Taglienti[1*], Maria Teresa Dell'Abate[2], Alessandra Ciampa[2], Laura Tomassoli[1], Giuliana Albanese[3], Luigi Sironi[4] and Antonio Tiberini[3]

[1]Council for Agricultural Research and Economics, Research Centre for Plant Protection and Certification (CREA-DC), Via C.G. Bertero 22 - 00156 Rome, Italy. [2]Council for Agricultural Research and Economics, Research Centre for Agriculture and Environment (CREA-AA), Via della Navicella 2/4 - 00184 Rome, Italy. [3]University "Mediterranea" of Reggio Calabria, Department of Agricultural Science, Località Feo di Vito - 89122 Reggio Calabria, Italy. [4]University of Milan, Department of Pharmaceutical Sciences, Via Balzaretti 9 – 20133 Milan, Italy.

**Corresponding author:*

Anna Taglienti, Research Centre for Plant Protection and Certification, Via C.G. Bertero 22 - 00156 Rome, Italy. Phone: +39 0682070228. Email: anna.taglienti@crea.gov.it

5,733 words

Short version of title: MRI ultrastructure of virus-infected onions.

Topic: Food Engineering, Materials Science, and Nanotechnology.

ABSTRACT: 'Rossa di Tropea' onion is a particular pink/red coloured onion cultivated in Calabria region (Southern Italy), representing one of the Italian most important vegetable crops granted with Protected Designation of Origin (PDO) and Protected Geographical Indication (PGI) trademarks. This

local cultivar is characterised by a high nutraceutical compounds content showing anti-inflammatory, anti-cholesterol, anticancer and antioxidant properties. As all vegetable crops and *Allium* spp., 'Rossa di Tropea' onion is affected by several viruses. Among these, the species *Onion yellow dwarf virus* (OYDV, genus *Potyvirus,* family *Potyviridae*), represents the most limiting biotic stress, inducing severe symptoms. OYDV effect on tissues architecture in whole bulbs was investigated using magnetic resonance microimaging (MRI) technique, which allows the interior of samples to be imaged non-invasively and non-destructively and yields quantitative information on physico-chemical parameters describing water mobility (T1 and T2 relaxation times). The use of such tool allowed to determine how OYDV alters plant physiology by inducing water accumulation in bulb tissues as well as causing ultra-structural modifications of cell wall, highlighted by MRI. All these effects resulted in an increase of free water in plant tissues, and consequently relevant water losses during post-harvest storage, seriously affecting bulb quality, marketability and shelf life.

Keywords: OYDV, virus disease, *Allium cepa*, MRI, proton relaxation.

1 Introduction

Plant-virus interaction, usually named infection, represents a sum of processes generated by susceptible cells in response to virus presence and replication (Van der Zaag, 1971), summarized as a complex of processes derived by an unending battle between host defense response and pathogen antagonising action (Poque et al., 2018).

Viruses use host cell resources to support their own reproduction (replication) and dissemination (cell-to-cell and long-distance movements) interfering with the normal plant processes, inducing physiological, biochemical and structural changes and anomalies, often leading to a clear symptomatology. These include micro/macroscopic or ultrastructural alterations as callose deposit

(Wolf, Deom, Beachy, & Lucas, 1991) and cell wall alteration (Lesemann, 1991).

The plant-virus interaction network understanding is becoming fundamental to better investigate the biology and the ecology role of plant viruses, in particular to elucidate the fine mechanism triggering a pathogenic relationship or, otherwise, an asymptomatic infection with no clear and direct effect on crop yield production. In fact, often latent or mild plant virus infections could lead to long term effect on product quality (i.e. during storage) and/or establish optimal conditions for secondary and post-harvest pathogens. Several plant-virus interaction models have been well studied and reported in literature (Culver & Padmanaban, 2007), regarding several crops and viruses. Among these, interaction model involving potyviruses is well documented, reporting data about infection effect under a molecular-biochemical and/or structural point of view (Poque et al., 2018; Elena & Rodrigo, 2012). However, few information is available about the species *Onion yellow dwarf virus*, a member of genus *Potyvirus* (Family *Potyviridae*), characterized by monopartite ssRNA (+) genome, reported infecting *Allium* spp. as garlic and onion. In particular, onion yellow dwarf virus (OYDV) was reported in onion for the first time in 1932 in Iowa (USA), and then worldwide spread (Dovas et al., 2001; Conci, Canavelli, & Lunello, 2003; Klukáčková, Navrátil, Veselá, Havránek, & Safářová, 2004; Abd El-Wahab, Elnagar, & El-Sheikh, 2009; Fayad-André, Dusi, & Resende, 2011; Katis, Maliogka, & Dovas, 2012; Kumar, Dhawan, & Mehra, 2012; Mohammed et al., 2013; Sevik & Akcura., 2013). In Italy, OYDV was reported in 1993 (Marani & Bertaccini, 1993) and later in 'Rossa di Tropea' onion (Parrella, De Stradis, Volvas, & Agosteo, 2005); it represents the most limiting biotic stress for this cultivar inducing, in natural infection, severe symptoms, as yellowing, dwarfing and stem twirling. Further, OYDV is reported to reduce, in early infections, bulbs weight and size up to 40 %, with a seed loss up to 50 % (Elnagar, El-Sheikh, & Abd El-Wahab, 2011). All these effects were reported analyzing early and natural infection, based on clear and distinguishable symptomatic plants (Elnagar et al., 2011). Conversely, few information is available about the effect of OYDV late infection and

when the virus is already present in plant tissues but at low titer and not able to trigger a clear symptomatological profile. When OYDV infection occurs in plants at mid-late phase of their vegetative cycle, corresponding to bulb formation, the symptoms are not so clear and/or plants are often asymptomatic (Henderson, 1935).'Rossa di Tropea' onion is a particular pink/red colored onion cultivated in Calabria region (Southern Italy), representing one of the Italian most important vegetable crops with Protected Designation of Origin (PDO) and Protected Geographical Indication (PGI) trademarks. In addition to its well-known organoleptic profile, this local cultivar is characterized by a high nutraceutical compounds content (i.e. phenolics, flavonoids, fructoligosaccharides, alk(en)yl cysteine sulphoxides) (Benitez et al., 2011) showing anti-inflammatory, anti-cholesterol, anticancer and antioxidant properties (Madaric et al., 2013; Kim, Kim, & Park, 2013). Long term storability is a key issue for onion quality: in order to cover the market needs for dry bulbs throughout the year, a huge amount of total production is stored before marketing, and water loss is the main limiting factor that determines storage duration (Petropoulos, Ntatsi, & Ferreira, 2017).

Magnetic resonance microimaging (MRI) is a non-destructive, non-invasive spectroscopic technique providing detailed morpho-structural images, information on the spatial distribution of proton density, relaxation parameters (spin-lattice relaxation time (T1) and spin-spin relaxation time (T2)), and self-diffusion coefficient inside the sample. Different MRI pulse sequences can be applied to modulate contrast factors (weighing) as a function of intrinsic molecular properties, such as nuclear relaxation times (T1 and T2) and diffusivity. In nuclear magnetic resonance relaxation, the energy acquired by a nucleus after its excitation by a radio frequency pulse is progressively lost; relaxation is related to structural variations, the overall molecular mobility, or the interactions undergone by the nucleus. The relaxation properties often provide complementary information and enhanced contrast of images (Mannina et al., 2017; Proietti et al., 2017); moreover, deduced T1 and T2 values are often used to describe the biological state of tissues (Abbott, 1999). Most interesting for applications on fruits and

vegetables, areas containing high mobility water are represented as brighter than surrounding tissues in MRI images, so that disorders, both abiotic and biotic, involving water distribution, can be visualized. Postharvest deterioration in 'Fuji' apples due to watercore, a physiological disorder affecting apple quality in which intercellular spaces are filled with liquid, was monitored by using MRI (Clark, MacFall, & Bieleski, 1998). Studies carried out on different plant species and pathogens found that T1-weighted images and proton distribution images of strawberries showed relaxation times and water proton densities shorter and higher, respectively, in samples infected by *Botrytis cinerea*, *Colletotrichum acutatum*, or *Phytophthora cactorum* (Maas, & Line, 1995); in potato, samples infected by several pathogens were clearly identified in MRI images (Snijder, Wastie, Glidewell, & Goodman, 1998): in particular, in T2-weighted images and T2-maps, the infected region contained relatively small amount of water, but of high mobility (Thybo, Jespersen, Laerke, & Stodkilde-Jorgensen, 2004). In onion, T2 distributions measured by NMR relaxometry were used to obtain information about cell membrane integrity of electrically processed (Ersus, Oztop, McCarthy, & Barrett, 2010) and high pressure and thermally treated bulbs (Gonzalez et al., 2010); these experiments were run on sliced disks or portions of scales to be put in the NMR tube; moreover, papery layers and the first fleshy scale were removed and samples were stored at 4°C until processing. In our MRI experiments, whole onion bulbs with no prior processing or cold storage were analyzed; hence, a comparison of relaxation times with the values reported in this work would not be appropriate. To date, at the best of our knowledge, there is not any published work on MRI analysis of onion. The non-destructive character of MRI technique is furthermore very important for shelf life and storability investigations on fruits and vegetables, because it allows to measure the same individual samples at all time points, avoiding errors due to biological variability and providing an actual representation of the evolution of the same tissues over storage time (Taglienti et al., 2011). Hence, MRI stands as the technique of choice for investigating internal structure and water status in biological and food tissues

(Ebrahimnejad, Ebrahimnejad, Salajegheh, & Barghi, 2018; Proietti et al., 2017). In view of the above, the objective of this work was to evaluate OYDV infection effect on 'Rossa di Tropea' onion by considering ultra-structural alterations and modifications of water status, which are relevant for bulb quality and shelf life aspects, as measured by MRI. This work represents, to the best of our knowledge, the first investigation on OYDV infection effects in 'Rossa di Tropea' onion at ultra-structural level by applying MRI.

2 Materials and methods

2.1 Plant material and experimental trial establishment

Plant material derived by a two-years experimental trial carried out in an insect-proof screen house at CREA-DC, Rome (Italy), using seeds of 'Rossa di Tropea' onion (biotype locally named *Mezza campana* or *Trottola*). The experimental trial provided a randomized block design including two theses (healthy-h and infected-OYDV), each thesis with three replicates (Figure 1). Totally, the trial involved 180 plants (each plant growing in one pot), 30 pots for each parcel and overall 6 parcels at 50 cm distance from one another. After harvest, bulbs were stored mimicking the conditions prescribed by the production protocol established by the 'Cipolla Rossa di Tropea PGI' consortium. Briefly, they were kept in a cardboard container in the dark at 20°C in a well-ventilated room.

The cultivation practices were those commonly performed in open field by farmers in 'Rossa di Tropea' onion production area. In particular, water and nutrient supplies were assured by daily irrigation, once every 12 h (20 l/m^2 per h), and 100 g/pot of diammonium phosphate in granules, respectively. In addition, fungicide treatments were performed by Rizolex® and Signum® applications, one pre-transplant (3 g/m^2) and two post-transplant, in a range of 10 days, (15 g/l), respectively.

143 Ninety days after transplant, when plants had five to seven leaves, an artificial inoculation was carried
144 out, in three out of six parcels, starting from fresh tissue material infected by OYDV isolate provided
145 by CREA-DC (Rome, Italy) virus collection. The infected crude extract, from leaves grounded in
146 phosphate buffer (0.1 M) in BIOREBA® bags (Reinach, Switzerland), was mechanically inoculated by
147 10 needle puncturing along two different leaves per plant. For each parcel, a new fresh inoculum was
148 prepared to avoid effect of a viral infectivity loss among the parcels.
149 For this study, three analytical time-points (10 plants for each time point of the 30 for each parcel),
150 were provided, overlapping the 'Rossa di Tropea' onion bulb production times: at harvesting time (t_0),
151 complete leaves drying (t_1) and after storage (t_2), corresponding approximately to 60, 90 and 150 d
152 post inoculation, respectively. In the meantime, they were stored as above described.
153 **2.2 Sanitary status verification**
154 Due to the late infection, leading to unclear symptom development, the assessment of virus inoculation
155 efficiency (OYDV thesis) and healthy status (h thesis) on plants was performed as follows: leaf
156 samples were collected from all 180 plants in the experimental trial and assayed by DAS-ELISA using
157 a kit specific for OYDV (Bioreba, Switzerland). Sampling and analysis were performed 21 days post
158 inoculum (*d.p.i.)*, 30 *d.p.i.* and at harvesting time (t_0).
159 **2.3 Magnetic Resonance Imaging (MRI) characterization**
160 Representative whole bulbs confirmed healthy and infected from the respective parcels were subjected
161 to MRI experiments to deduce morphological and physico-chemical parameters able to describe the
162 internal arrangement of vegetal tissues and the water mobility herein. Due to the instrumentation used,
163 involving costly facilities and machine time-consuming issues, a limited number of 8 samples each
164 year (4 healthy and 4 infected) was selected for this study. The preliminary investigation, aimed at a
165 first comparison between healthy and infected bulbs and assessing features showing differences, was
166 performed on a selection of representative bulbs of the first year of experimental trial. In particular,

167 healthy (4 samples) and OYDV infected (4 samples) bulbs after storage stage (t_2), having mean
168 diameter less than 70 mm (maximum dimension allowed by the instrumental sample holder), were
169 selected for the analysis. Then, MRI measurements were performed on both healthy (4 samples) and
170 OYDV infected (4 samples) samples derived by the second year of the experimental trial in all three
171 sampling time-points, i.e. t_0, t_1 and t_2.
172 Multi Slide Multi Echo (MSME) experiments were recorded on a Bruker Avance 300 MHz Super
173 Wide Bore (Bruker Italia srl, Milan, Italy) at CREA-AA in Rome for the preliminary survey on
174 samples from the first year trial; samples of the second year were analyzed on a Bruker Avance 200
175 MHz Super Wide Bore (Bruker Italia srl, Milan, Italy) at Department of Pharmacological and
176 Biomolecular Sciences in Milan. Experimental conditions were maintained the same on both
177 measurements sets, in particular: two conventional spin echo sequences (T1 and T2-weighted MSME
178 experiments) were used. In T2-weighted MSME the following acquisition parameters were used:
179 single slice, number of scans 1, slice thickness 1.0 mm, echo time TE = 10.0 ms, repetition time TR =
180 3000 ms, matrix size = 128 × 128, spectral width 100 kHz, field of view (FOV) = 40 x 40 mm,
181 excitation pulse = sinc 3. The T1-weighted MSME sequence was acquired with single slice; number of
182 scans = 1, slice thickness 1.0 mm; TE = 10.0 ms; TR = 3000 ms; matrix size = 128 × 128; spectral
183 width 100 kHz; FOV = 40 x 40 mm. Before each spectroscopic measurement, the bulb was let to
184 thermally equilibrate at 22 °C for 30 min within the sample holder.
185 To calculate T1 and T2 relaxation times, in the first year a preliminary investigation was performed
186 limited on t_2 samples: ten circular regions of interest were randomly drawn on the axial section images
187 of the onion tissue, and T1 and T2 of each region were calculated using image sequence analysis (ISA)
188 tool package (Paravision 3.0.2, Bruker), which uses T1sat reported in Equation (1) and T2vtr reported
189 in Equation (2) fit functions to extract relaxation time values.
190

$$y=A+C(1-\exp(-t/T1) \quad (1)$$

$$y= A+C*\exp(-t/T2) \quad (2)$$

In the second year, 7 circular regions of interest (ROIs) named ROI 1 to ROI 6 (radially from core to external skin layer, Figure 2) across the onion tissues and a ROI 7 comprising the whole onion axial section area, which is larger and more representative, were drawn and analyzed as above described.

T1 and T2-weighted images were also analyzed by ImageJ 1.8.0 software (NIH, U.S.A) to perform greyscale analysis. Intensities of the acquired image were reduced to a scale from 0 to 255, the first value corresponding to full black and the second to complete white, which is the usual scale of a digitized image. The whole sample area was selected and parameterized images were used to build histograms according to pixel intensities.

T1 and T2 calculation and greyscale analysis of T1 and T2-weighted images are methods related to each other, the main differences being that the latter accounts contemporarily for T1 or T2 values and water amount and allows the selection of areas far apart to each other in the image. For a correct use of greyscale analysis, values must be referred to the same surface area in different samples; hence, the final values were obtained by dividing for the total number of pixels constituting the images and normalizing for the maximum. Furthermore, MRI images analyzed by ImageJ were obtained by using the same acquisition and processing parameters.

2.4 Statistical analysis

Analysis of variance (ANOVA, $p \leq 0.05$), was carried out on calculated T1 and T2 relaxation times, to highlight significant differences between healthy and OYVD infected bulbs at t_2 stage for the first year trial, and at t_0, t_1 and t_2 for the second year trial. Significantly different groups were identified on the basis of ANOVA using Fisher's least significant difference (LSD) test: for the first year trial, two groups (healthy and infected) were subjected to ANOVA, while for the second year six groups

(healthy and infected for each of the three time points) were subjected to ANOVA; in the latter case, the significant differences highlighted the alteration of the selected variable (T1 or T2) with respect to both storage time and infection condition.

3 Results

3.1 MRI preliminary analysis

MRI images of onion bulbs sections obtained at t_2 in the first year showed morphological differences between healthy and OYDV infected samples: a thickening of the fleshy leaves epidermis in the internal and external discs in the infected bulbs with respect to healthy control was observed in both T1 and T2-weighed experiments (Figure 3, left panel); correspondingly, T2 measurements also showed significantly different values depending on the phytosanitary status. OYDV infected samples had higher (+14.4 %) mean values of T2 than the healthy control, indicating changes in the mobility of water inside the plant tissues ($p<0.01$); T1 values showed no significant differences between healthy and infected groups (Figure 3, right panel).

3.2 MRI measurements during post-harvest

On the basis of the preliminary screening reported in Section 3.1, which was limited both in sampling time (t_2) and method (randomly chosen areas within the section image, irrespective of radial position and specific tissue), in the second year the investigation was extended to t_0, t_1 and t_2 sampling times and an established grid method was used to draw the ROIs, taking into account the different concentric tissues in onion bulb section.

From the MRI images obtained at t_0, t_1 and t_2 on a selection of healthy and infected bulbs in the second year (Figure 4), we obtained information on the onion internal morphology and its evolution over time, and consequently it was possible to observe significant changes in the OYDV infected samples with respect to healthy control during the storage period. As in the preliminary experiments at t_2 of the first

239 year, both the images weighted in T1 and T2 showed a thickening of the fleshy leaves epidermis in the
240 infected bulbs with respect to healthy control; the change was noticeable since t_1 and was even more
241 evident at t_2; such images were a valuable tool for investigating cellular membrane integrity and in
242 particular physico-chemical changes in onion tissues. The calculated mean values of T1 and T2 of each
243 ROI also showed significant differences between healthy and OYDV infected groups, the differences
244 increasing with storage time (Table 1); in particular, T1 mean values of infected group were around
245 +40 % with respect to healthy control at t_2 in ROIs 2, 3, 4 and 6, with a maximum increase of +48 % in
246 ROI 2 (representing the inner leaf layer covering the core) and a 30 % increase in ROI 7 (representing
247 the overall section area of the bulb). OYDV infected group showed even higher increments with
248 respect to healthy group in T2 mean values at t_2 in ROIs 2 and 3, with a maximum increase of 68 % in
249 ROI 3 (representing the second inner leaf layer covering the core) and an increase of 43 % in ROI 7.
250 ROI 1 (representing the bulb core) and ROI 5 (representing the fourth inner leaf layer covering the
251 core) showed no significant differences related to phytosanitary status in all the 3 sampling stages,
252 while in ROI 6 (representing the fifth inner leaf layer covering the core) we measured significant
253 differences of T1 but not of T2.
254 The plot of T1 vs T2 mean values of ROI 2, 3, 4 and 7 (Figure 5), clearly describes a separation
255 between the two groups of samples, highlighting the possibility to further apply discriminant analysis
256 on a larger set of samples, when available.
257 Histograms referring to greyscale analysis of T1 and T2-weighted images of each sample at t_0 are
258 shown in Figure S1; the same trend was observed for t_1 and t_2 sampling times. Greyscale analysis was
259 performed in order to promptly read the images in terms of relaxation times; in fact, high intensity
260 values on the grey scale histogram are related to bright pixels (long T1 or T2) while low intensity
261 values refer to dark pixels (short T1 or T2); also the mono-exponential decay of relaxation functions
262 was confirmed by greyscale analysis, as only one maximum was observed for each histogram and only

263 one proton component of water, thus of T1 and T2 values, was provided by MRI analysis in our
264 samples.

265
266

267 ## 4 Discussion

268 The study of proton relaxation behavior in healthy and infected bulbs over storage time allows to
269 deduce that it was affected by viral infection.

270 Longitudinal relaxation time (T1, due to spin-lattice relaxation processes) and transverse relaxation
271 time (T2, due to spin-spin relaxation processes) describe the properties of water in different locations
272 or compartments within the tissue and the interaction of water with macromolecules (Snaar & Van As,
273 1992). The water exchange rates between these compartments are controlled by the water permeability
274 of the intervening membranes (Van Der Weerd, Claessens, Efde, & Van As, 2002; Scheenen,
275 Heemskerk, de Jager, Vergeldt, & Van, 2002) and T2 of the different compartments will depend on the
276 compartment morphology, permeability of surrounding membranes, exchange with macromolecules
277 (Van As 2007; Van Duynhoven, Voda, Witek, & Van As, 2010); hence, in this study, it is not
278 straightforward to attribute T2 evolution to a specific factor correlated to virus infection. Moreover,
279 there is no published work reporting T1 and T2 of onion tissues as measured by MRI in the literature
280 for comparison with values described in our study. For all these reasons, only a speculation on most
281 likely explanation of relaxation values evolution with progressing disease is possible, also taking into
282 account the acknowledged mechanisms of virus infection and its effects on vegetable tissues.

283 Generally, T2 values are used to describe the biological state of tissues by interpreting it as the ration
284 of bound water to free water (Abbott, 1999). Highest T2 values are expected in those conditions where
285 spinning protons dephase slowly, as occurs in free water, thus the significantly higher T2 values
286 observed in the infected onion samples may be explained by release of intracellular fluids and water

287 with greater mobility and proton density following a partial lysis of cellular tissues; this interpretation
288 is supported by the knowledge of virus infection mechanisms inducing structural changes as cell wall
289 alteration, degradation of chloroplast membrane and alterations of cytoplasm and organelle structure
290 (Lesemann, 1991).
291 Moreover, the higher T1 values in infected onion tissues could be associated with changes in
292 polysaccharides, as well as in protein structure (defolding, aggregation), which can affect their
293 functionality and the texture/structure of onion tissues, as the longitudinal dephasing T1 is mainly due
294 to spin-lattice relaxation processes. Callose deposit, which is a well known phenomenon associated
295 with viral pathogenesis (Wolf et al., 1991) may be involved in T1 changes.
296 Whereas differences in both T1 and T2 parameters are able to distinguish infected from healthy
297 onions, the wider differences in T2 values between healthy and OYDV infected groups seem to
298 indicate that the major process in stored virus-infected onion bulbs is water release within tissues,
299 which is accompanied by slight morphological modifications in the spaces between contiguous fleshy
300 leaves, as shown by the MRI images.
301 The selection of appropriate areas for ROIs sampling, corresponding to the different concentric fleshy
302 leaves of the onion bulb epidermis, allowed to better highlight the tissues particularly and/or early
303 affected by OYDV infection in terms of ultra-structural alteration due to water status change. In fact,
304 onion epidermis consists of concentric bulb fleshy leaves which exert both protective action (external
305 discs) and protein reserve (internal discs) of the bulb and the alteration of outer or inner layers may
306 reflect in impairing different physiological functions over time.
307 In particular, the increase of T1 observed in infected group was detected even since t_1 in internal disc
308 ROI 2, while was limited to t_2 storage time for external discs (ROIs 3 and 4); this may suggest that the
309 damage of the virus infection at ultra-structural level starts from the inner leaves (excluding the core
310 ROI 1) and propagates to the outer layers with storage time; hence, the protein reserve function is

311 weakened at early storage time, while the protective action is spoiled only in long term storage.
312 A similar trend was observed for T2 increase of infected group, which was significant ($p<0.01$) since t_1
313 in internal discs ROI 2 and 3, involving the whole axial section of the bulb (ROI 7) only at t_2.
314 These results indicate that OYDV infection could determine an increase of free water content in bulbs.
315 In fact, in particular at the end of the storage period (t_2) bulbs show a higher T2, which generally
316 accounts for a great amount of free water. This parameter is reported to be fundamental in correct
317 storage conditions and to prevent post-harvest pathogens infection (Petropoulos et al., 2017, Gubb &
318 MacTanish 2002). It could be assumed that an increase in free water in OYDV-infected bulb could
319 affect long-term storage criteria and conditions leading to an overall decrease of product quality, in
320 particular for its shelf life.
321

322 ## 6 Conclusion

323 MRI proved to be a powerful tool to study the effects of OYDV infection on onion bulbs
324 ultrastructure. Images highlighted alterations in onion tissues as thickening of the fleshy leaves
325 epidermis in the internal and external discs in the infected bulbs; the measurement of relaxation
326 parameters T1 and T2 also evidenced differences between healthy and virus-infected samples. Both
327 these effects were of increasing importance during storage.
328

329 **Acknowledgments**
330 This study was carried out in the frame of the project: *Study on Interaction between Onion yellow*
331 *dwarf virus and nutraceutical compounds of "Rossa di Tropea" onion*, (SIR-MIUR grant – SIORTO-
332 RBSI149LD5) funded by Italian Ministry of University, Education and Research - MIUR, in the frame
333 of *Scientific Independence of young Researcher* - SIR initiative. The founding source was not involved
334 in study design, analysis and interpretation of data, writing the report and decision to submit the article

for publication.

The authors declare that they have no conflict of interest.

Authors Contributions

ATi, LT, MTDA and GA conceived and designed the work. ATi, AC, ATa and LS performed the experiments and acquired the data. ATa performed statistical analysis. ATi, ATa, AC, MTDA, LT and GA wrote the manuscript. All authors read and approved the manuscript.

Supplementary information

Supplementary files should be published online as such.

References

Abbott, J.A. (1999). Quality measurement of fruits and vegetables. *Postharvest biology and technology*, 15, 207-225. 10.1016/S0925-5214(98)00086-6

Abd El-Wahab, A.S., Elnagr. S., & El-Sheikh, M.A.K. (2009). Incidence of aphid-borne Onion yellow dwarf virus (OYDV) in alliaceae crops and associated weeds in Egypt. *4th Conference on Recent Technologies in Agriculture*, 21-33.

Benitez, V., Molla, E., Martin-Cabrejas, A., Lopez-Andreu, F.J., Downes, K., Terry, L.A., & Esteban, R.M. (2011) Study of bioactive compound content in different onion sections. *Plant foods for human nutrition*, 66(1), 48-57.

Conci, V.C., Canavelli, A., & Lunello, P. (2003). Yield losses associated with virus–infected garlic plants during five successive years. *Plant Disease*, 87, 1411.

Culver, J.N., & Padmanabhan, M.S. (2007). Virus-induced disease: altering host physiology one interaction at a time. *Annual Review of Phytopathology*, 45, 221-243. 10.1146/annurev.phyto.45.062806.094422

Clark, C.J., MacFall, J.S., & Bieleski, R.L. (1998) Loss of watercore from 'Fuji' apple observed by magnetic resonance imaging. *Scientia Horticolturae*, 73(4), 213–227.

Dovas, C.I., Hatziloucas, E., Salomon, R., Barg, E., Shiboleth, Y., & Katis, N.I. (2001) Incidence of viruses infecting *Allium* spp. in Greece. *European Journal of Plant pathology*, 107, 677-684.

Ebrahimnejad, H., Ebrahimnejad, H, Salajegheh, A., & Barghi, H. (2018). Use of Magnetic Resonance Imaging in Food Quality Control: A Review. *Journal of Biomedical Physics and Engineering,* 8(1), 127–132.

Elena, S. F., & Rodrigo, G. (2012) Towards and integrated molecular model of plant-virus interactions. *Current Opinion in Virology*, 2(6), 719-724. 10.1016/j.coviro.2012.09.004

Elnagar, S., El-Sheikh, M. A. K., & Abd El-Wahab, A.S. (2011). Effect of Natural infection with Onion yellow dwarf virus (OYDV) on yield of onion and garlic crops in Egypt. *Journal of Life Science*, 5, 634-638.

Ersus, S., Oztop, M. H., McCarthy, M. J., & Barrett, D. M. (2010). Disintegration efficiency of Pulsed Electric Field induced effects on onion (*Allium cepa* L.) tissues as a function of pulse protocol and determination of cell integrity by ^{1}H-NMR relaxometry. *Journal of Food Science*, 75(7), E444-E452. 10.1111/j.1750-3841.2010.01769.x

Fayad-André, M. de S., Dusi, A. N., & Resende, R. O. (2011). Spread of viruses in garlic fields cultivated under different agricultural production systems in Brazil. *Tropical Plant Pathology*, 36, 341–349. 10.1590/S1982-56762011000600001

Gonzalez, M. E., Barrett, D. M., McCarthy, M. J., Vergeldt, F. J., Gerkema, E., Matser, A. M., & Van As, H. (2010). ^{1}H-NMR study of the impact of high pressure and thermal processing on cell membrane integrity of onions. *Journal of Food Science*, 75(7), E417-E425. 10.1111/j.1750-3841.2010.01766.x

Gubb, I. R., & MacTavish, H. S. (2002). Onion pre- and post-harvest considerations. In: Rabinowitch, H.D., Currah, L. (eds.) *Allium Crop Sciences: Recent Advances*. CAB Int.: Wallingford, UK, 233–266.

Henderson, W. J. (1935). Yellow Dwarf, a virus disease of Onions, and its control. *Research Bulletin (Iowa Agriculture and Home Economics Experiment Station)*, 16(188), Article 1.

Katis, N.I., Maliogka, V.I., & Dovas, C.I. (2012). Viruses of the genus Allium in the Mediterranean Region. In: Lecoq H., Loebenstein G., (eds.) *Viruses and Virus Diseases of Vegetables in the Mediterranean Basin*. Academic Press, San Diego, CA, USA, 163–208.

Kim, J., Kim, J.S., & Park E. (2013). Cytotoxic and anti-infilammatory effects of onion peel extract on lipopolysaccharide stimulated human colon carcinoma cells. *Food and Chemical Toxicology*, 62, 199-204. 10.1016/j.fct.2013.08.045

Klukáčková, J., Navrátil, M., Veselá, M., Havránek, P., & Safářová, D. (2004). Occurrence of garlic viruses in the Czech Republic. Proceedings Conference organized at Slovak Agricultural University in Nitra, Slovakia. *Acta Fytotechnica et Zootechnica*, 7, 126-128.

Kumar, P., Dhawan, P., & Mehra, R. (2012). Symptoms and losses caused by *Onion yellow dwarf virus* and *Iris yellow spot virus* diseases of onion crop in Northern India. *Journal of Mycology and Plant Pathology*, 42(1), 153-160.

Lesemann, D.E. (1991). Specific Cytological Alterations in Virus-Infected Plant Cells. In: Mendgen K., Lesemann D.E. (ed) *Electron Microscopy of Plant Pathogens*. Springer, Berlin, Heidelberg.

Maas, J. L., & Line, M. J. (1995). Nuclear magnetic resonance (NMR) inversion recovery spin echo microimaging of fungus infections in strawberry fruit. *Acta Horticulturae*, 398, 241-248. 10.17660/ActaHortic.1995.398.25

Madaric, A., Kadrabova, J., Krajcovicova-Kudlackova, M., Valachovicova, M., Spustova, V., Mislanova, C., Kajaba, I., & Blazicek, P. (2013). The effect of bioactive complex of quercetin, selenium, catechins and curcumin on cardiovascular risk markers in healthy population after a two months consumption. *Bratislavské lekárske listy*, 114(2), 84-87.

Mannina, L., Sobolev, A. P., Aru, V. *et al*., (2017) NMR Methodologies in Food Analysis. Chapter 5 In: Locatelli M., Celia, C. (eds.) *Analytical Chemistry - Developments, Applications and Challenges in Food Analysis*. Nova Science Publishers, Inc.: 103-156 ISBN: 978-1-53612-267-1

Marani, F., & Bertaccini, A. (1983). Virosi delle liliaceae ortive: cipolla, aglio, porro. In: *Le virosi delle piante ortive*. Reda Editore per l'Agricoltura, Rome, Italy, 104-111.

Mohammed, H.S., Zicca, S., Manglli, A., Mohamed, M.E., El Siddig, M.A.R., El Hussein, A.A., & Tomassoli, L. (2013). Occurrence and phylogenetic analysis of potyviruses, carlaviruses and allexiviruses in garlic in Sudan. *Journal of Phytopathology*, 161(9), 642-650. 10.1111/jph.12115

Parrella, G., De Stradis, A., Volvas, C., & Agosteo, G.E. (2005). Outbreaks of *Onion yellow dwarf virus* (OYDV) on onion crops in Calabria (Southern Italy). *Journal of Plant Pathology*, 87(4), 302.

Petropoulos, S.A, Ntatsi, G., & Ferreira, I.C.F.R. (2017). Long-term storage of onion and the factors that affect its quality: A critical review. *Food Reviews International*, 33(1), 62-83. 10.1080/87559129.2015.1137312

452 Poque, S., Wu, H.W., Huang, C.H., Cheng, H.W., Hu, H.W., Yang, J.Y., Wang, D., & Yeh, S.D.
453 (2018). Potyviral gene-silencing suppressor NcPro interacts with salicylic acid (SA)-Binding
454 Protein 3 to weaken SA-mediated defense response. *Molecular plant-microbe interactions*, 31(1),
455 86-100. 10.1094/MPMI-06-17-0128-FI
456
457 Proietti, N., Capitani, D., Aru, V. et al. (2017) NMR Methodologies in Food Analysis: Part B. Chapter
458 7. In: Locatelli, M., Celia, C. (eds.) *Analytical Chemistry - Developments, Applications and*
459 *Challenges in Food Analysis* Nova Science Publishers, Inc., 255-295. ISBN: 978-1-53612-267-1.
460
461 Scheenen, T., Heemskerk, A., de Jager, A., Vergeldt, F., & Van, A.H. (2002). Functional imaging of
462 plants: a nuclear magnetic resonance study of a cucumber plant. *Biophysical Journal*, 82, 481–92.
463 10.1016/S0006-3495(02)75413-1
464
465 Sevik, M.A., & Akcura, C. (2013). Viruses occurring in onion crop in Amasya province, the major
466 onion producing region in Turkey. *Indian Journal of Virology*, 24, 78-81. 10.1007/s13337-012-
467 0114-z
468
469 Snaar, J.E.M., & Van As, H. (1992). A NMR method for the simultaneous measurement of
470 compartmentalized spin–lattice and spin–spin relaxation times in multi compartment systems.
471 *Journal of Magnetic Resonance*, 99, 139–148.
472
473 Snijder, A.J., Wastie, R.L., Glidewell, S.M., & Goodman, B.A. (1996). Free radicals and other
474 paramagnetic ions in interactions between fungal pathogens and potato tubers. *Biochemical Society*
475 *Transactions*, 24, 442–446.

Taglienti, A., Ritota, M., Cozzolino, S., Sequi, P., Valentini, M., Conte, L., & Terlizzi, M. (2011). MRI characterization of new kiwifruit selections. *Acta Horticolturae,* 931, 145-155. 10.17660/ActaHortic.2011.913.17

Thybo, A. K., Jespersen, S. N., Laerke, P. E., & Stodkilde-Jorgensen, H. J. (2004). Nondestructive detection of internal bruise and spraing disease symptoms in potatoes using magnetic resonance imaging. *Magnetic Resonance Imaging*, 22, 1311. 10.1016/j.mri.2004.08.022

Van As, H. (2007). Intact plant MRI for the study of cell water relations, membrane permeability, cell-to-cell and long distance water transport. *Journal of Experimental Botany*, 58, 743–56. 10.1093/jxb/erl157

Van Der Weerd, L., Claessens, M. M. A. E., Efde, C., & Van As, H. (2002). Nuclear magnetic resonance imaging of permeability changes in plants during osmotic stress. *Plant Cell Environment*, 25, 1539–49. 10.1046/j.1365-3040.2002.00934.x

Van der Zaag, D.E. (1971). Symptoms of virus diseases in plants. *Potato Research*, 14, 102. 10.1007/BF02355936

Van Duynhoven, J., Voda, A., Witek, M., & Van As, H. (2010). Time domain NMR applied to food products. *Annual Reports NMR on Spectroscopy,* 69, 145 –197. 10.1016/S0066-4103(10)69003-5

Wolf, S., Deom, C. M., Beachy, R., & Lucas, W. J. (1991). Plasmodesmatal function is probed using transgenic tobacco plants that express a virus movement protein. *The Plant Cell*, 3, 593-604. 10.1105/tpc.3.6.593

Table 1. Calculated T1 and T2 mean values of ROI 2, 3, 4, 6 and 7 from MRI axial section images of healthy and OYDV-infected bulbs, and ANOVA analysis.

ROI	**group**	**n**	**T1**			**T2**		
			t0	t1	t2	t0	t1	t2
2	h	4	1671±234	1786± 224	1458±447	55.6±4.9	51.3± 5.8	47.4±9.0
	OYDV	4	1880±72	1841±134	2153±342	56.6±2.5	62.7±7.4	68.8±12.1
	ANOVA			*			*	
	F value			2.87			4.11	
ROI	**group**	**n**	**T1**			**T2**		
			t0	t1	t2	t0	t1	t2
3	h	4	1792±233	1856±131	1795±342	54.2±12.3	52.4±8.2	48.6±4.8
	OYDV	4	2113±103	2058±65	2590±474	62.9±5.7	71.4±11.6	81.5±22.0
	ANOVA			**			**	
	F value			5.19			4.29	
ROI	**group**	**n**	**T1**			**T2**		
			t0	t1	t2	t0	t1	t2
4	h	4	1807±207	1948±158	1969±380	61.5±11.2	59.7±11.3	57.1±8.5
	OYDV	4	1995±110	2278±150	2565±391	66.6±1.2	71.2±8.7	90.2±18.5
	ANOVA			**			**	
	F value			4.63			4.71	
ROI	**group**	**n**	**T1**			**T2**		
			t0	t1	t2	t0	t1	t2
6	h	4	1747±280	1767±206	1916±167	70.2±10.8	76.1±12.0	81.5±28.2
	OYDV	4	1724±284	2163±306	2750±653	67.5±6.3	79.7±5.2	82.3±11.6
	ANOVA			**			n.s.	
	F value			5.06			-	

ROI	group	n	T1			T2		
			t0	t1	t2	t0	t1	t2
7	h	4	1740±189	1649±172	1721±160	61.4±6.1	60.4±10.2	57.7±7.7
	OYDV	4	1954±104	1649±82	2243±249	63.4±2.0	69.4±5.3	82.9±15.0
	ANOVA			**			**	
	F value			7.34			4.54	

515 **Figure 1.** Experimental scheme (randomized blocks) of trial. In A, D and E blocks the plants were
516 inoculated with OYDV; in B, C and F blocks the plants were untreated (not inoculated) representing
517 the healthy controls h. Plants at the inoculation time (bottom left corner), plants at harvesting time
518 (bottom right corner).
519

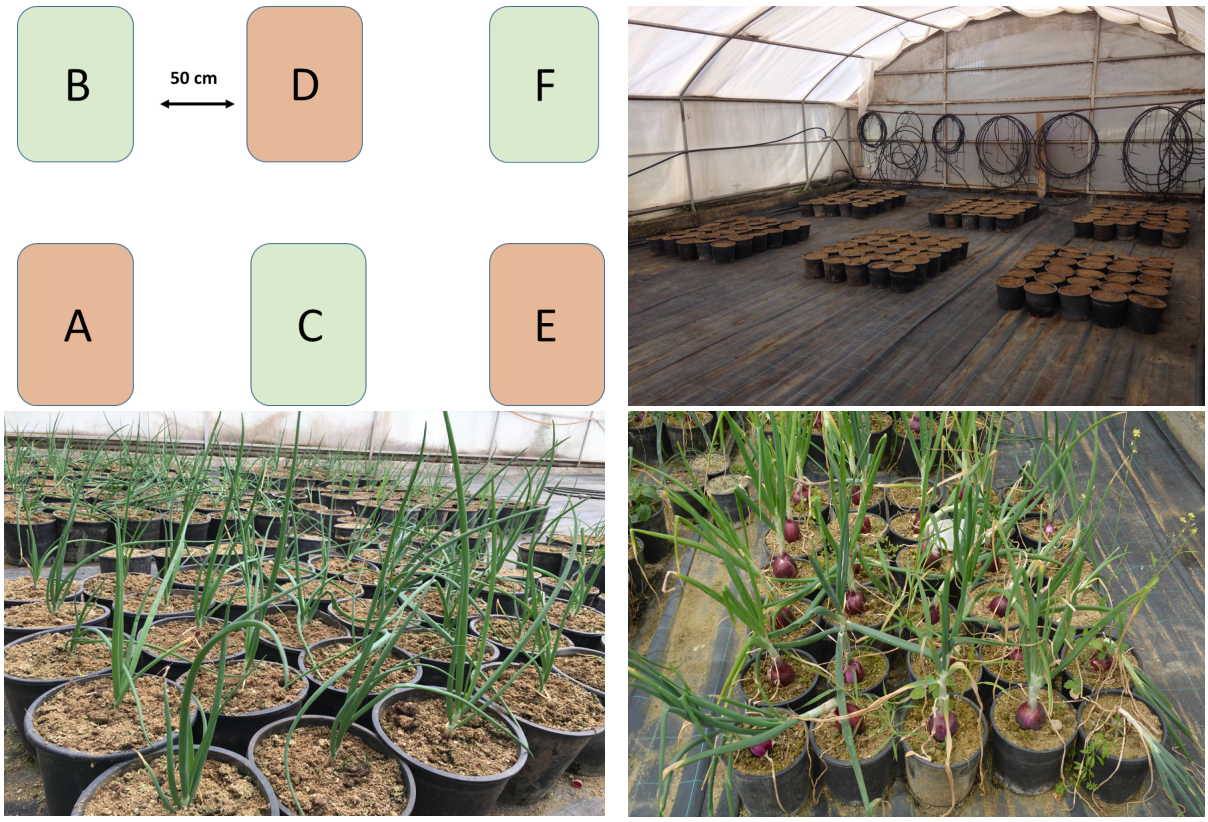

520

Figure 2. Drawing of the 7 regions of interest (ROIs) across the axial section of the onion bulb image for T1 and T2 calculation.

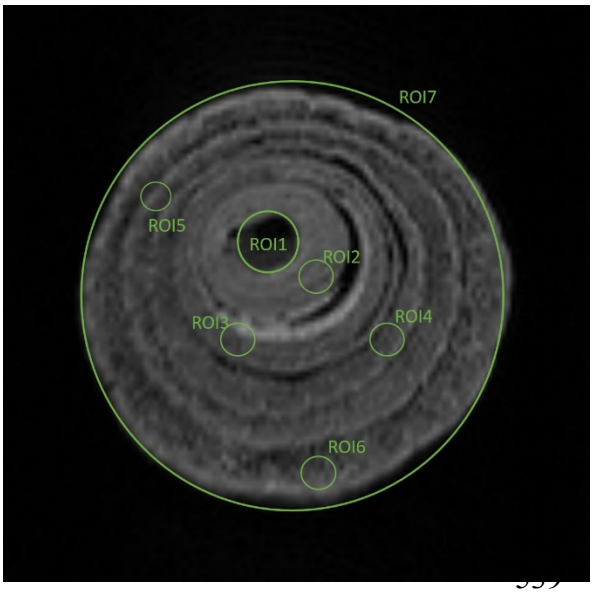

541 **Figure 3.** MRI images of axial section of '*Rossa di Tropea*' onion bulbs; msme -T2 [(A)-healthy and
542 (B)-infected samples] and msme-T1 images [(C)-healthy and (D)- infected samples] (left panel); T1
543 and T2 mean values obtained for healthy and infected samples. ** = ANOVA test significant at p>0.01.
544

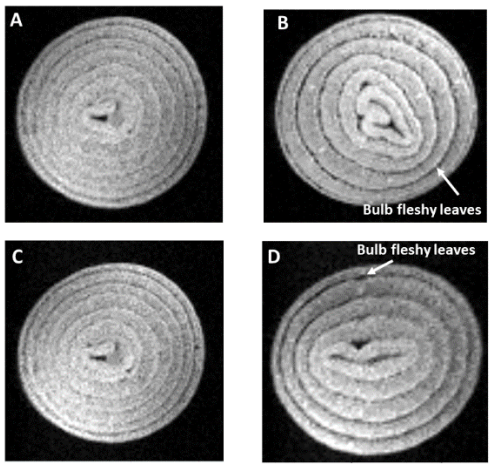

Group	n	T2
healthy	4	51.78±4.5
infected	4	60.47±7.6
ANOVA		**
F value		41.73

552

553 **Figure 4.** MRI images of axial section of healthy (h) and OYDV-infected (OYDV) '*Rossa di Tropea'*

554 onion bulbs at t_0, t_1 and t_2 sampling times obtained by msme-T1 and msme-T2 experiments.

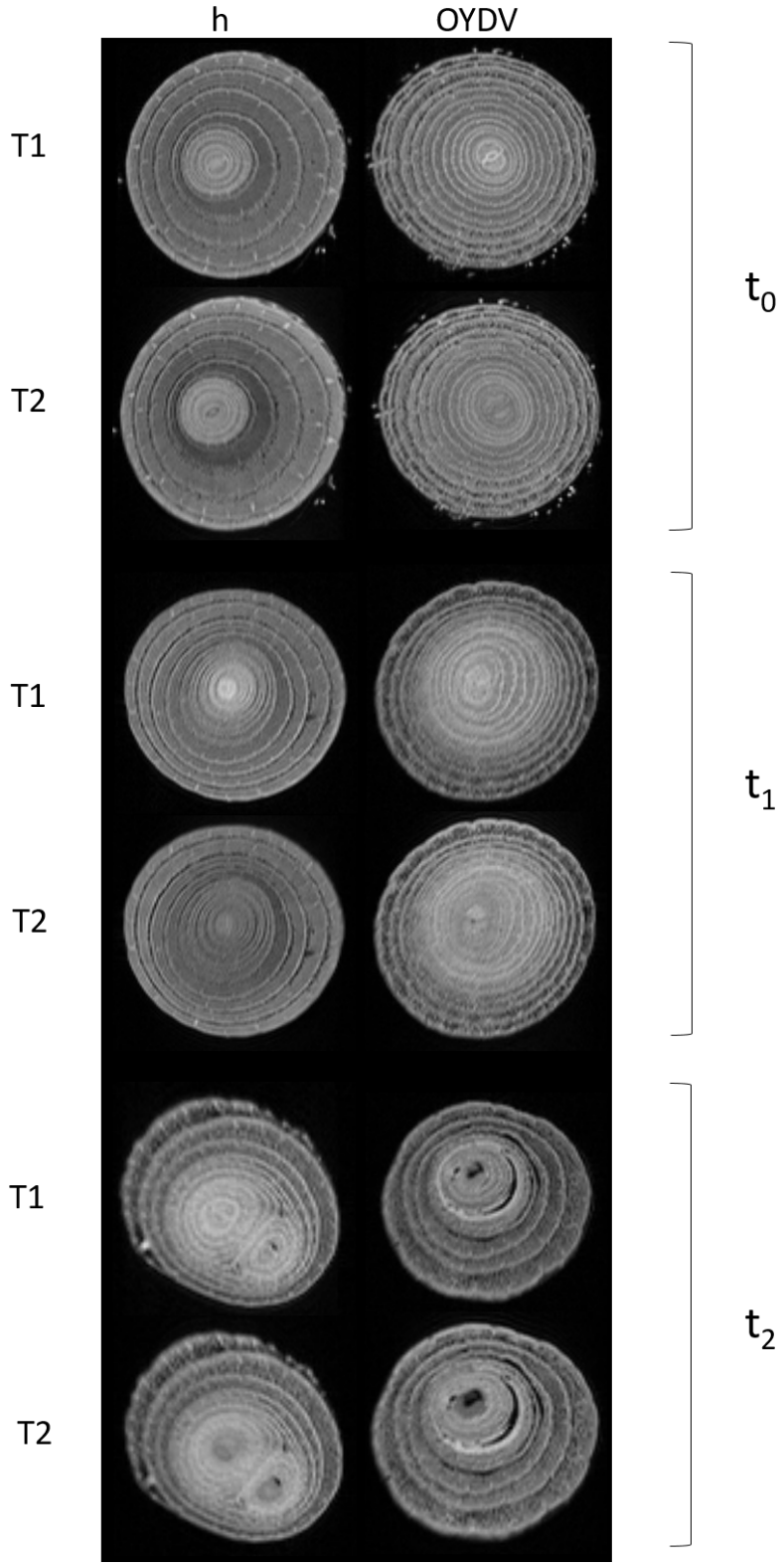

555

Figure 5. T1 vs. T2 plot of ROI 2 (panel A), ROI 3 (panel B), ROI 4 (panel C), ROI 7 (panel D).